High-fidelity Numerical Simulations of Collapsing Cavitation Bubbles Near Solid and Elastically Deformable Objects

Mauro Rodriguez[1], Shahaboddin Beig[1], Zhen Xu[2], and Eric Johnsen[1]

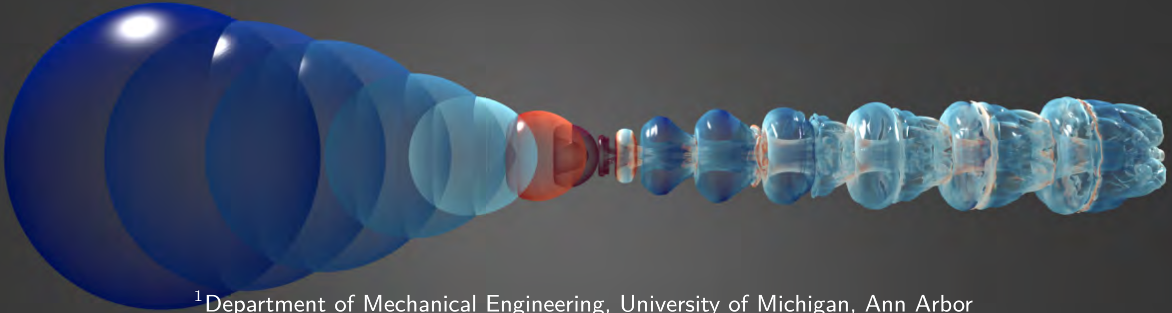

[1]Department of Mechanical Engineering, University of Michigan, Ann Arbor
[2]Department of Biomedical Engineering, University of Michigan, Ann Arbor

Blue Waters Symposium 2019
Sunriver, Oregon, June 3-6

This research is part of the Blue Waters sustained-petascale computing project, which is supported by the National Science Foundation (awards OCI-0725070 and ACI-1238993) and the state of Illinois.

We Used Blue Waters to Predict Cavitation Impacts Loads

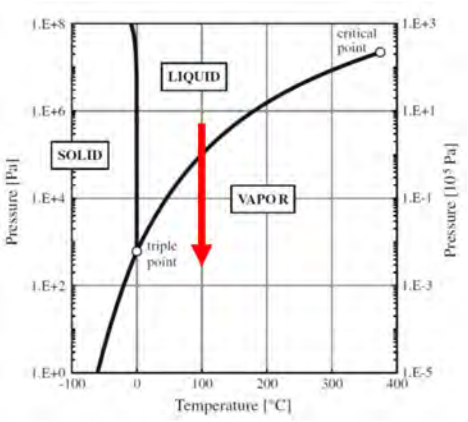

Pressure-driven vaporization

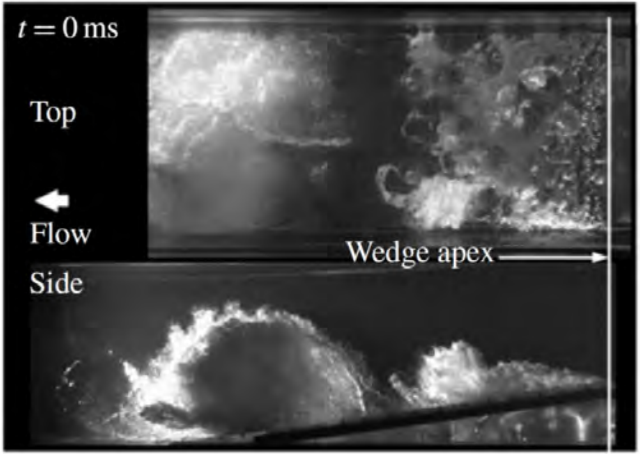

Ganesh et al. 2016

We Used Blue Waters to Predict Cavitation Impacts Loads

Brennen 1994

Four stages of cavitation damage in metals (Franc et al. 2011): small vapor structure formation, impact loading from bubble collapse, pitting, and failure

Bubbles Respond to Their Environment by Oscillating in Volume

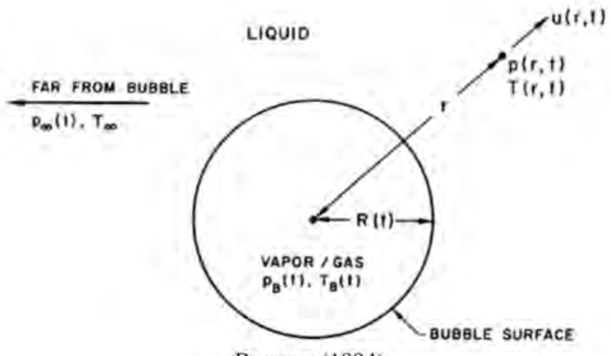

Brennen (1994)

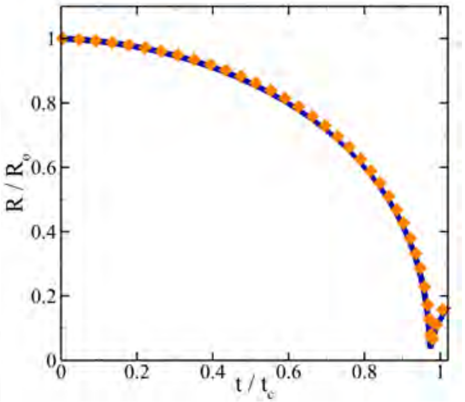

State of the art compressible, multiphase framework can simulate inertially-driven collapses and agrees with theory (Alahyari Beig, 2018)

Bubbles Respond to Their Environment by Oscillating in Volume

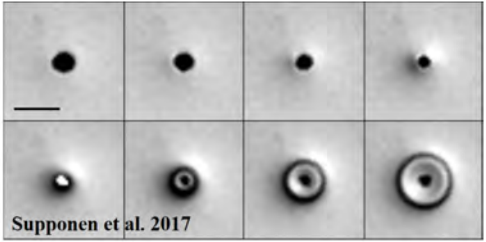

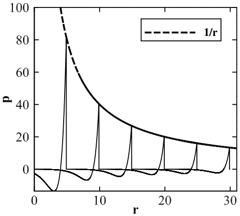

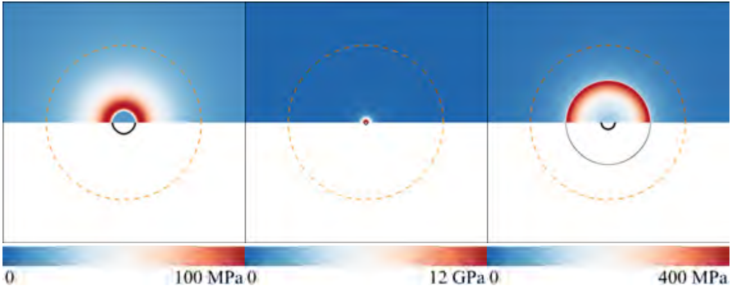

In extreme cases, the bubbles implode and emit an outward propagating shock wave into the surroundings

Inertially-driven Bubble Collapse Damage Near Rigid Surfaces

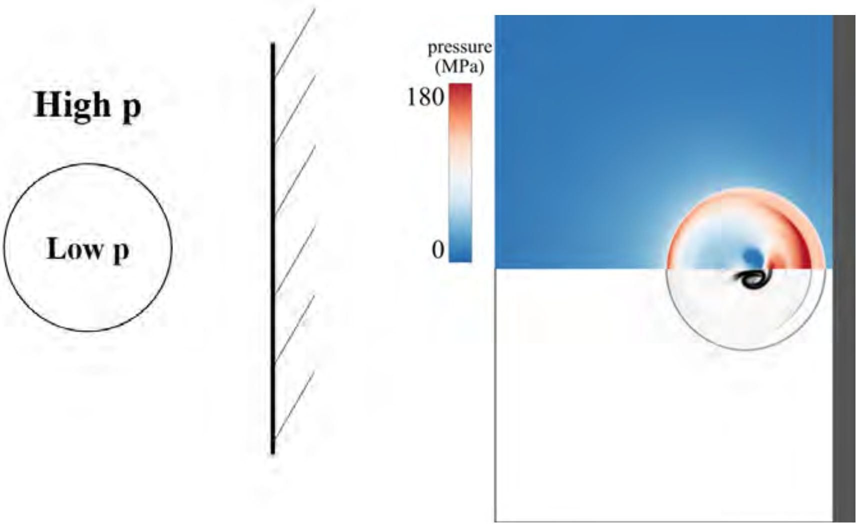

Inertially-driven bubble collapse asymmetrically near a wall

$$p^* = \frac{p_{mw}}{\rho_l a_l \sqrt{\Delta p/\rho_l}}$$

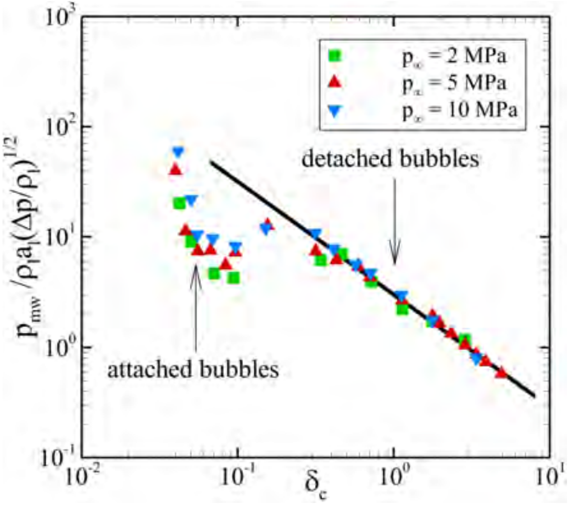

With the appropriate scaling the maximum pressures along the wall collapse to a single curve (Alahyari Beig, 2018)

Cavitation-induced Damage Near Rigid/Soft Media is Poorly Understood

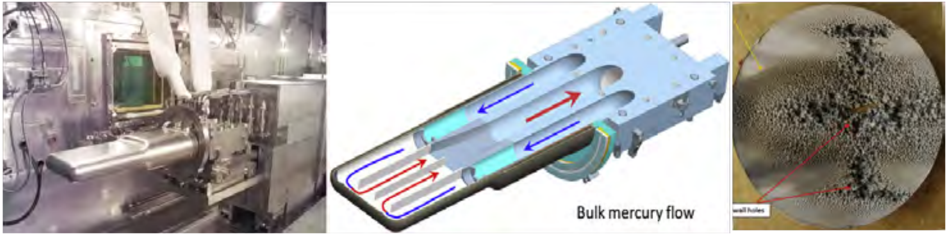

Cavitation in liquid mercury inhibits experimentation of neutron scattering experiments

neutrons2.ornl.gov/facilities (left), Riemer et al. 2014 (middle,right)

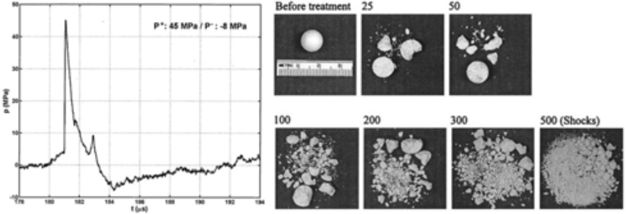

Extracorporeal shock wave lithotripsy and similar tools used to treat stones, Zhu et al. 2002

Cavitation leads to more effective stone comminution

Research Objective: Leverage high-fidelity CFD with Blue Waters to understand the cavitation-induced damage/erosion mechanisms in and near rigid/soft media

I. Non-linear bubble-bubble interactions near a rigid wall (bakg/baxd)
II. Effect of confinement on inertial bubble collapse (basr)
III. Shock-induced bubble collapse near elastic media (basr)

Numerical Model & Computational Approach

- Hyperbolic-Parabolic system of equations for multi-component, thermal Zener model

$$\frac{\partial}{\partial \mathrm{t}}\begin{bmatrix}\rho^{(k)}\alpha^{(k)}\\ \rho u_i\\ E\\ \rho\tau_{il}^{e}\\ \rho\xi_{ilm}\end{bmatrix}+\frac{\partial}{\partial \mathrm{x}_j}\begin{bmatrix}\rho^{(k)}\alpha^{(k)}u_j\\ \rho u_i u_j+p\delta_{ij}-\tau_{ij}^{e}\\ u_j(E+p-\tau_{ij}^{e})\\ \rho\tau_{il}^{e}u_j\\ \rho\xi_{ilm}u_j\end{bmatrix}=\begin{bmatrix}0\\ \tau_{ij,j}^{v}\\ (u_i\tau_{ij}^{v}+(\kappa T)_{,j})_{,j}\\ \mathrm{S}_{il}^{e}\\ \mathrm{S}_{il}^{\xi}\end{bmatrix}\begin{matrix}\text{Mass}\\ \text{Momentum}\\ \text{Energy}\\ \text{Stress}\\ \text{Memory}\end{matrix}$$

In-house high-order, solution-adaptive computational framework is used

$$\left.\frac{dU}{dt}\right|_i+\frac{F_{i+1/2}(U)-F_{i-1/2}(U)}{\Delta x}=D_i(U)+S_i(U)$$

- Time marching: 4^{th}-order accurate explicit Runge-Kutta
- Smooth regions: 4^{th}-order accurate finite-difference central scheme
- Discontinuous regions: 5^{th}-order accurate WENO (Jiang & Shu, 1996) w/ sensor with one of two upwinding approaches (preventing spurious errors)
  - HLL (Alahyari Beig et al., JCP 2015)
  - AUSM^{+}-up (Rodriguez et al. Shock Waves 2019)
- Constitutive eq.: Hypoelastic model using Lie derivative (Rodriguez & Johnsen, JCP 2019)

High-fidelity simulation needs

- Superior peta-scale performance
- Large simulations : >1 billion computational points for 13+ variables
- Multiple two-day simulations for each simulation case

Strong scaling

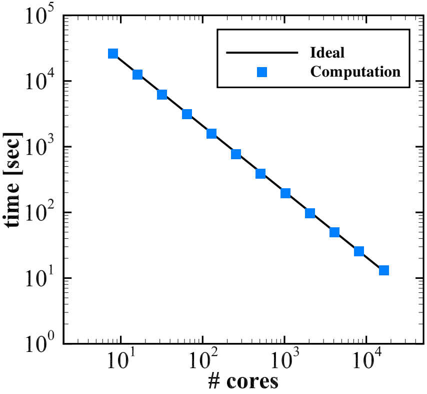

Weak scaling

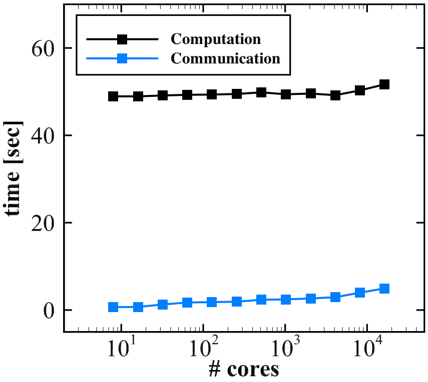

Research Objective: Leverage high-fidelity CFD with Blue Waters to understand the cavitation-induced damage/erosion mechanisms in and near rigid/soft media

I. Non-linear bubble-bubble interactions near a rigid wall (bakg/baxd) ☑

- PI: Eric Johnsen, Co-PIs: S. A. Beig, M. Rodriguez
- Publications: two archived papers and two archived papers in preparation
- Thesis: S. A. Beig (2018)
- Four conferences talks

II. Effect of confinement on inertial bubble collapse (basr) ☑

III. Shock-induced bubble collapse near (visco)elastic media (basr) ☑

- PI: Zhen Xu, Co-PIs: M. Rodriguez, S. A. Beig
- Publications: two archived papers in preparation
- Thesis: M. Rodriguez (2018)
- Three conferences talks

I. Rayleigh Collapse of Twin Bubbles near a Rigid Wall

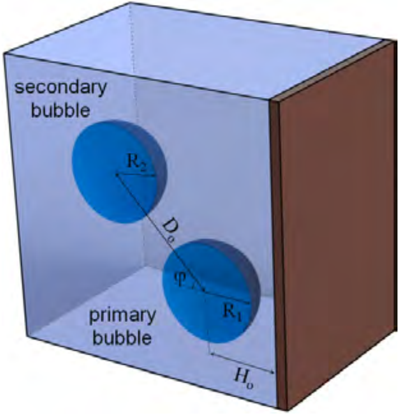

- $\mathrm{R_o} = 500\ \mu m$ (initial radius)
- $\mathrm{p}_\infty = 2, 5,$ and 10 MPa
- $\mathrm{p_{gas}} = 3550$ Pa
- $\delta_o = \mathrm{H/R_o}$, initial distance from $\mathrm{Wall_L}$
- ϕ, angle from the horizontal
- γ_o, distance between the bubbles
- Resolution $=$ 192 ppibr $\approx$ 1-2.5 billion points

Stress unit $=$ 5.2 kPa, Temperature unit $=$ 300K, Time unit $=$ 1.1 μs

Medium	ρ [kg/m^3]	a [m/s]	n [-/-]	B [MPa]	b [m^3/kg]
Water, vapor	0.027	439.6	1.47	0	0
Water, liquid	1051	1613	1.19	702.8	6.61E-4

Single-bubble vs Twin-bubble - Qualitative Behavior

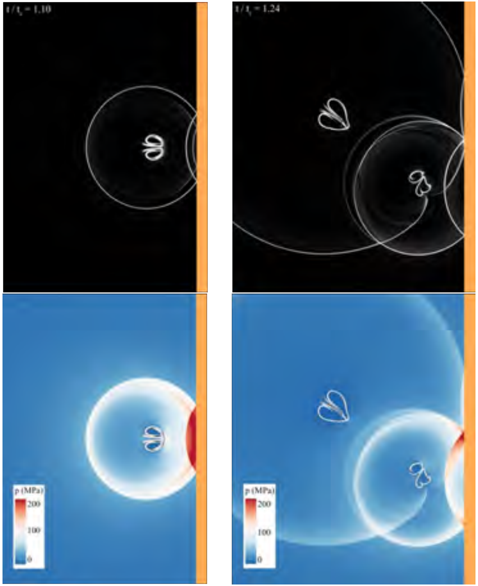

- $p_\infty = 5$ MPa, $\delta_o = 1.5$
- $\gamma_o = 3.5$, $\phi = 45^o$
- Contours of density gradient (top) and pressure (bottom)
- Secondary bubble forms a re-entrant jet towards the primary bubble
- Water-hammer shock wave propagates towards primary bubble
- Primary bubble's collapse is enhanced and distorted as collapses

Maximum and Average Wall Pressure - Twin-bubble

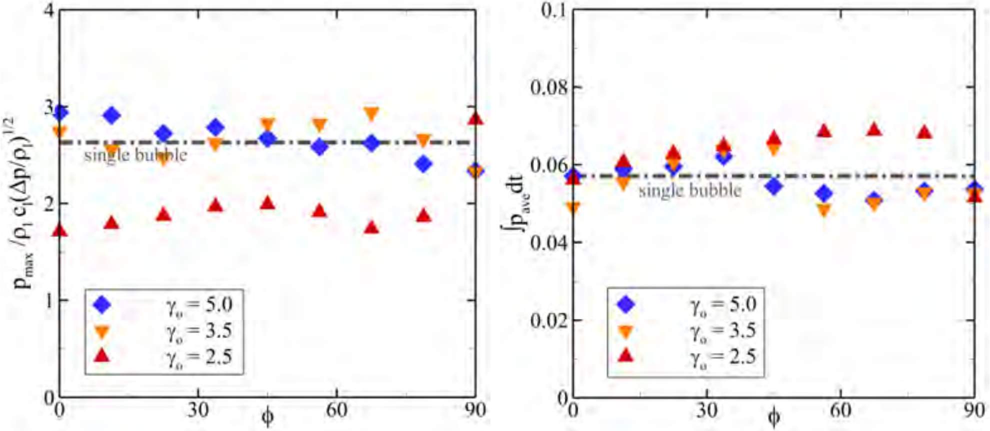

- Farther bubble produce higher maximum pressures (impact load) relative to the single wall
- However, closer bubbles produces larger impulse load on the wall relative to the wall
- Scientific impact: Gaining fundamental understanding of the non-linear bubble-bubble interactions towards developing high-fidelity bubble clouds models

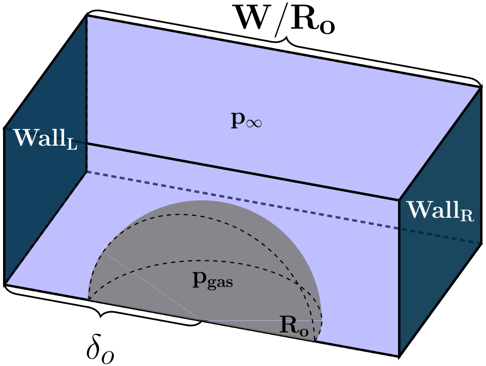

- $R_o = 500\ \mu m$ (initial radius)
- $p_\infty = 2, 5,$ and 10 MPa
- $p_{gas} = 3550$ Pa
- $\delta_o = H/R_o$, initial distance from $Wall_L$
- δ_c, bubble collapse distance from $Wall_L$
- Resolution = 192 ppibr $\approx$ 0.45 billion points

Stress unit = 5.2 kPa, Temperature unit = 300K, Time unit = 1.1 μs

Medium	ρ [kg/m^3]	a [m/s]	n [-/-]	B [MPa]	b [m^3/kg]
Water, vapor	0.027	439.6	1.47	0	0
Water, liquid	1051	1613	1.19	702.8	6.61E-4

Rayleigh Collapse of a Bubble in a Channel - Wall Pressure

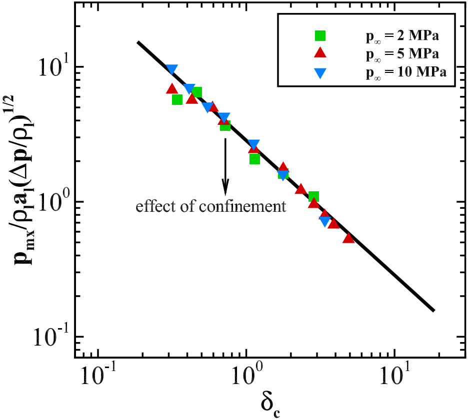

- Data collapses to a single curve of slope -1 when considering δ_c
- Hypothesis: Confinement reduces the maximum wall pressures due to the restricted fluid motion, i.e., entrainment of fluid at collapse & jet formation

Rayleigh Collapse of a Bubble in a Channel - Wall Pressure w/ Confinement

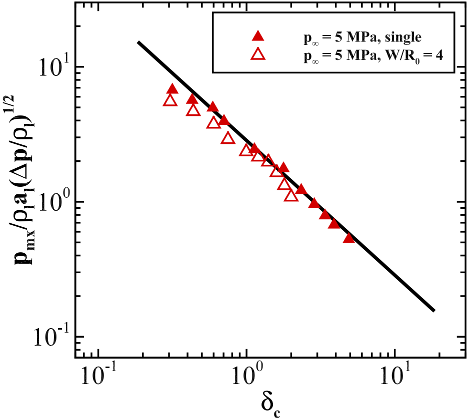

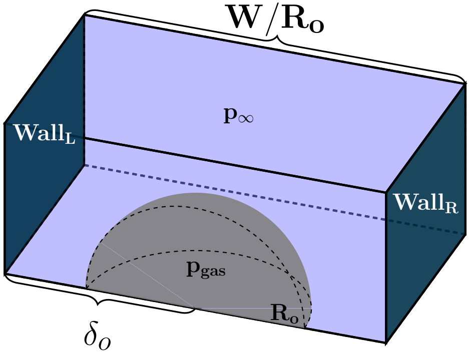

- Weaker pressure response in the channel although smaller minimum volume are achieved at collapse due to limited re-entrant jet(s) formation

Rayleigh Collapse of a Bubble in a Channel - Wall Pressure w/ Confinement

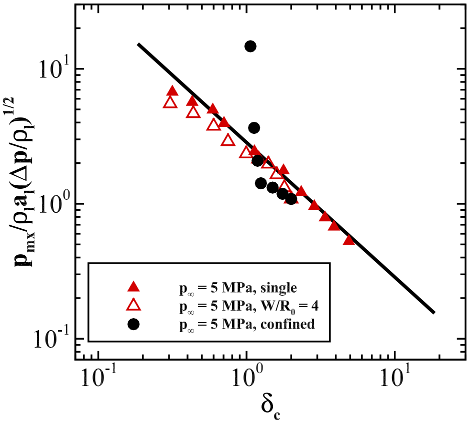

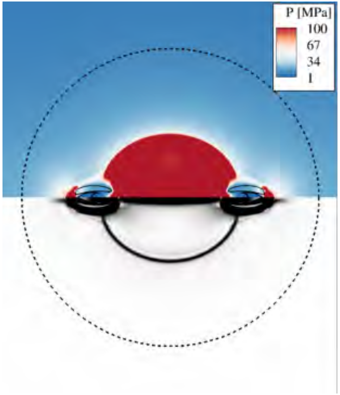

- Bubble's re-entrant jet formation is further restricted in the confined cases leading to weaker outward propagating water-hammer shock waves that interact with the nearby wall
- For the $W/R_o < 5/4$, the water-hammer shock from the vertical re-entrant jet strengthens the collapse the vortex ring and the wall pressure response

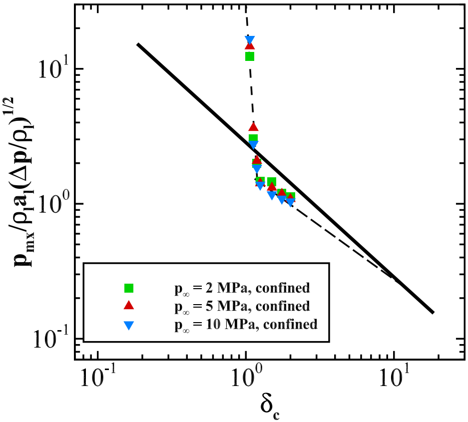

- Data collapses along a single curve with $\mathrm{W/R_o} < 5/4$ being the critical confinement ratio for vertical re-entrant jet formation
- Scientific impact: Continuing modeling efforts to develop scaling relationships to predict impact loads (and transition) from confined inertial bubble collapse

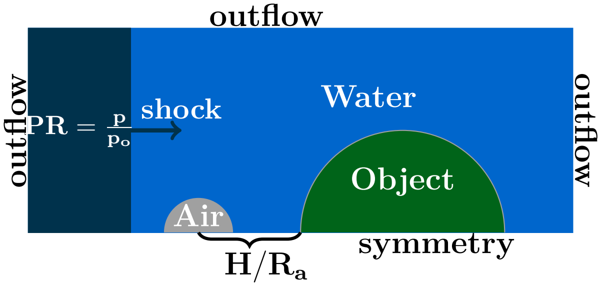

- $\mathrm{R_a} = 100\ \mu m$ (initial radius)
- $\mathrm{p} = 30$ MPa (lithotrisy pulse)
- $\mathrm{H/R_a} = 1.25$, bubble to stone distance
- Stone to bubble ratios = 5, 10, 15, and 20
- Resolution = 48 ppibr ≈ 1-3.1 billion points

Stress unit = 5.2 kPa, Temperature unit = 300K, Time unit = 1.1 μs

Medium	ρ [kg/m^3]	c_L [m/s]	μ [Pa·s]	G [Pa]
Air	1	376	1.8×10^{-5}	-
Water	1000	1570	10^{-3}	-
Model kidney stone	1700	3500	-	3×10^{9}

Model kidney stone properties comparable to those in Zhong et al. (1993) for kidney stones

Hypothesis: Shock-bubble interaction shields the stone from experiencing maximum tension in the stone relative to the shock-stone case

Shock-induced Bubble Collapse Near a Spherical Kidney Stone

Shock-stone interaction

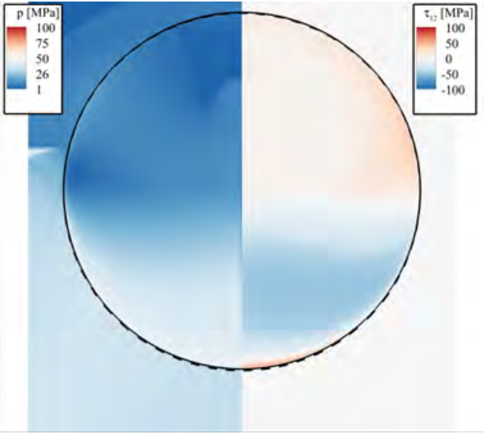

Shock-bubble-stone interaction

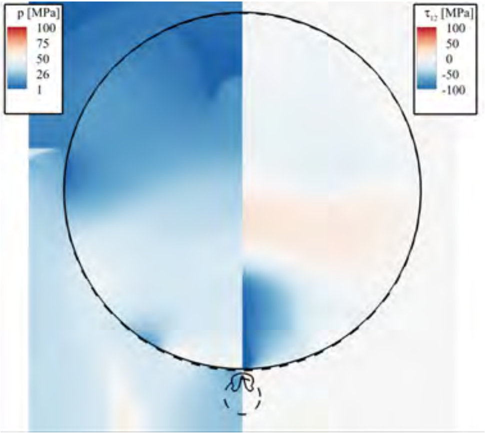

- Tension waves across the stone surface from the shock wave and reflected transmitted shock wave (cusp) are observed
- Bubble's shock wave limits the tension stress magnitude in the stone from the shock wave

Shock-induced Bubble Collapse Near a Spherical Kidney Stone

Shock-stone interaction

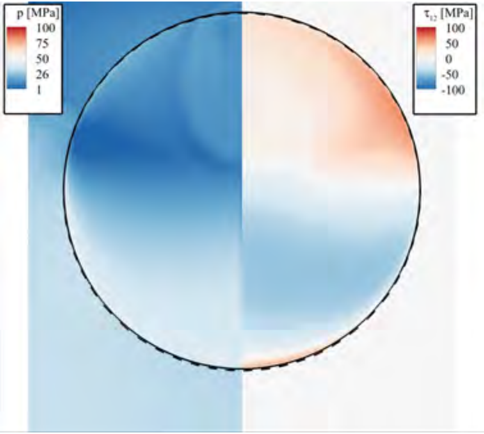

Shock-bubble-stone interaction

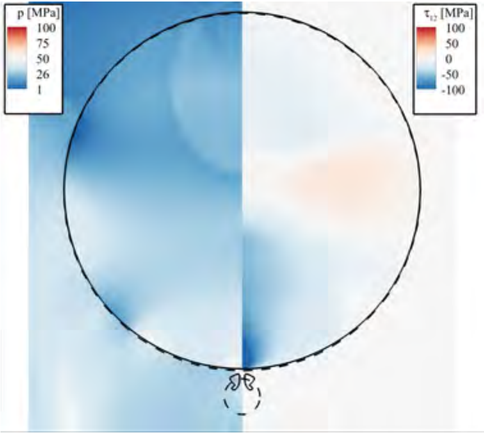

- Scientific impact: Quantifying three regimes for effective stone comminution: shock only (large stones), bubble-shock (medium stones), bubble only (stone)

Conclusions & Broader Impacts

- Studying bubble collapse dynamics in various context and configurations to predict impact loads in cavitation erosion
- Key result: Conducted high-fidelity, peta-scale simulations uniquely possible at Blue Waters
  - Quantifying/modeling bubble-bubble interactions near a rigid wall
  - Developing scaling to predict impact loads from confined cavitation
  - Quantifying the regimes of bubble-shock interactions for effective stone comminution
- Future work
  - Multiple bubbles (bubble cloud modeling)
  - Bubble collapsing in a corner

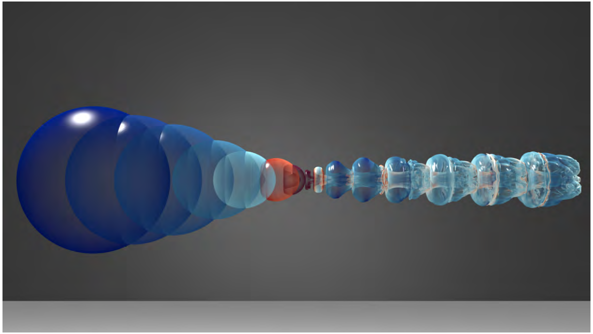

Key image: Highly-resolved volume rendering/time lapse of bubble collapsing near a rigid wall colored by temperature

BLUE WATERS

This research is part of the Blue Waters sustained-petascale computing project, which is supported by the National Science Foundation (awards OCI-0725070 and ACI-1238993) and the state of Illinois.

BACKUP SLIDES

- Novel multi-component, thermal Zener numerical model

$$\frac{\partial}{\partial \mathrm{t}}\begin{bmatrix} \rho \\ \rho^{(k)}\alpha^{(k)} \\ \rho u_i \\ E \\ \rho\tau_{ij}^{(e)} \\ \rho\xi_{ij}^{(l)} \end{bmatrix} + \frac{\partial}{\partial \mathrm{x}_j}\begin{bmatrix} \rho u_j \\ \rho^{(k)}\alpha^{(k)}u_j \\ \rho u_i u_j + p\delta_{ij} - \tau_{ij}^{(e)} \\ u_j(E + p - \tau_{ij}^{(e)}) \\ \rho\tau_{ij}^{(e)}u_j \\ \rho\xi_{ij}^{(l)}u_j \end{bmatrix} = \begin{bmatrix} 0 \\ 0 \\ \tau_{ij,j}^{(v)} \\ (u_i\tau_{ij}^{(v)} + (\kappa T)_{,j})_{,j} \\ \mathrm{S}_{ij}^{(e)} \\ \mathrm{S}_{ij}^{(\xi)} \end{bmatrix} \begin{array}{l} \text{Mass} \\ \\ \text{Momentum} \\ \text{Energy} \\ \text{Stress} \\ \text{Memory} \end{array}$$

$$\frac{\partial\alpha^{(k)}}{\partial \mathrm{t}} + u_j\frac{\partial\alpha^{(k)}}{\partial \mathrm{x}_j} = \Gamma\frac{\partial u_j}{\partial \mathrm{x}_j}, \qquad \Gamma = \alpha^{(1)}\alpha^{(2)}\frac{\rho^{(2)}(a^{(2)})^2 - \rho^{(1)}(a^{(1)})^2}{\alpha^{(1)}\rho^{(2)}(a^{(2)})^2 + \alpha^{(2)}\rho^{(1)}(a^{(1)})^2}$$

- **Lie derivative implementation**: Consistent, finite strains (Altmeyer et al., 2015)

$$\mathrm{S}_{ij}^{(e)} = \rho\left[\tau_{kj}^{(e)}\frac{\partial u_i}{\partial x_j} + \tau_{ik}^{(e)}\frac{\partial u_j}{\partial x_k} + \tau_{ij}^{(e)}\frac{\partial u_k}{\partial x_k} + 2\left(G\dot{\epsilon}_{ij}^{(d)} - \frac{1}{3}\tau_{kl}^{(e)}\dot{\epsilon}_{kl}\delta_{ij}\right) + \sum_{l}^{N_r}\xi_{ij}^{(l)}\right],$$

$$\mathrm{S}_{ij}^{(\xi)} = \rho\left[\tau_{kj}^{(e)}\frac{\partial u_i}{\partial x_j} + \tau_{ik}^{(e)}\frac{\partial u_j}{\partial x_k} + \tau_{ij}^{(e)}\frac{\partial u_k}{\partial x_k} - \theta_l\left(2\varsigma_l G_r\dot{\epsilon}_{ij}^{(d)} - \frac{1}{3}\tau_{kl}^{(e)}\dot{\epsilon}_{kl}\delta_{ij} + \xi_{ij}^{(l)}\right)\right]$$

In a rectangular Cartesian frame, Lie derivative is equal to Truesdell derivative